Molecular mechanisms of antibiotic resistance: QM/MM modelling of deacylation in a class A β-lactamase

Johannes C. Hermann,[a,b] Lars Ridder,[a,c] Hans-Dieter Höltje[d] and Adrian J. Mulholland*[a]

Received 13th September 2005, Accepted 14th November 2005
First published as an Advance Article on the web 9th December 2005
DOI: 10.1039/b512969a

Modelling of the first step of the deacylation reaction of benzylpenicllin in the *E. coli* TEM1 β-lactamase (with B3LYP/6-31G + (d)//AM1-CHARMM22 quantum mechanics/molecular mechanics methods) shows that a mechanism in which Glu166 acts as the base to deprotonate a conserved water molecule is both energetically and structurally consistent with experimental data; the results may assist the design of new antibiotics and β-lactamase inhibitors.

Bacterial resistance against antibiotics is a severe and growing problem in antibacterial therapy.[1] β-Lactamases, and particularly the class A family of these enzymes, are the most common form of resistance against the very important group of β-lactam antibiotics. Breakdown of the β-lactam bond (the defining structural element of these drugs, indispensable for their antibiotic effect) happens in two main steps. The first step is acylation of Ser70[2] by the antibiotic, to form an acylenzyme intermediate. The next stage is deacylation, in which the acylenzyme (AE) is hydrolysed. The former β-lactam compound—now cleaved and without any antibiotic potency—is then released.[3] Depending on the antibiotic, either acylation or deacylation can be the rate-determining step for the whole enzymic reaction.[4] For the widely-studied model β-lactam antibiotic, benzylpenicillin (which is investigated here), the kinetic constants of acylation and deacylation are believed to be similar for the *E. coli* TEM1 class A enzyme, indicating that both reaction steps contribute to the overall rate of the reaction.[4]

Combined quantum mechanics/molecular mechanics (QM/MM) methods are a good approach to the investigation of enzyme-catalysed reaction mechanisms. We have recently applied QM/MM methods to establish the mechanism of acylation of the TEM1 β-lactamase with benzylpenicillin: the calculations identified Glu166 as the base.[5,6] Here we have applied similar, well-tested methods to the first step of the proposed deacylation mechanism, the formation of the tetrahedral intermediate (TI).[7] In this deacylation mechanism, Glu166 removes a proton from a structurally conserved water molecule, activating it for nucleophilic attack on the acylenzyme (AE) (Scheme 1). We find that Glu166 activates the nucleophile for attack on the carbonyl group in deacylation, as it does in acylation. The catalytic water molecule is vital in both steps, either as a 'proton transfer station' (in acylation; it accepts a proton from Ser70 while being deprotonated by Glu166) or as the nucleophile (in deacylation). A tetrahedral intermediate (TI) is formed in both steps.

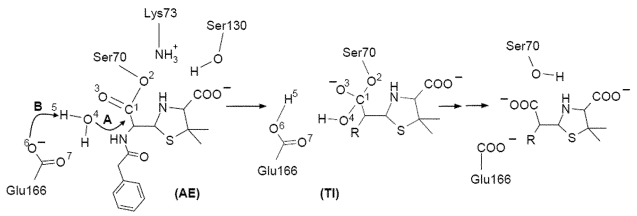

Scheme 1 Deacylation mechanism leading from the acylenzyme (AE) to the tetrahedral intermediate (TI) and to the cleaved antibiotic. The reaction processes of the first step, which is modelled here, are marked A and B, and atom numbers are shown for some important atoms (see text for details).

The TI reacts to give the cleaved benzylpenicillin and the free enzyme. Formation of the TI is likely to be the process with the highest energy barrier in deacylation, in analogy to acylation.[6] In acylation, the AE is formed from the TI by several proton transfers, which regenerate unprotonated Glu166. These involve Lys73 and Ser130 as proton shuttle residues, and have relatively low barriers. The TIs of both reaction steps, and the transition states for their formation, are structurally similar, and are (as we show here) stabilized by analogous interactions with the protein.

The starting point for QM/MM modelling of deacylation was the crystal structure of E166N mutant TEM1 β-lactamase from *E. coli* in complex with benzylpenicillin (PDB[8] code 1FQG[9]). This was altered to regain the wild type. It was relaxed, solvated and truncated to an 18 Å radius sphere (as described in detail in ref. 6). QM/MM calculations[10] were then performed with the CHARMM software package (version 27b2).[11] In a QM/MM calculation, it is necessary to select atoms for treatment at the quantum mechanical level. The QM region in this case was large (70 atoms, with a charge of −1 in total). It contained the entire substrate (benzylpenicillin), the catalytic water molecule and sidechain atoms of Ser70, Lys73, Ser130 and Glu166. The remainder of the system (3216 water and protein atoms) was described at the molecular mechanical level by the CHARMM22-forcefield.[12] Structures were optimized (see below) at the semiempirical AM1-CHARMM22 QM/MM level[10] Electrostatic, van der Waals and bonded interactions between the QM and MM regions are included. The AE (the product of acylation and the starting geometry for deacylation) was generated by QM/MM modelling as described in ref. 6. This optimized structure should be representative of the reaction: no large scale conformational changes are believed to occur.[6] High-level energy corrections (using hybrid density functional theory) were applied to obtain more reliable reaction energetics, as described below.[13] This

[a]*School of Chemistry, University of Bristol, Bristol, BS8 1TS, U.K*
[b]*Department of Pharmaceutical Chemistry, University of California San Francisco, QB3, 1700 4th Street, San Francisco, California, 94143*
[c]*Molecular Design & Informatics, N.V. Organon, P.O. Box 20, 5340 BH, Oss, The Netherlands*
[d]*Institut für Pharmazeutische Chemie, Heinrich-Heine Universität Düsseldorf, Universitätsstrasse 1, 40225, Düsseldorf, Germany*

QM/MM method has been found to perform well, in our studies of the acylation reaction, and for other enzymes.[14] Four hydrogen (HQ-type) 'link atoms'[15] were introduced to saturate the shells of QM-atoms covalently bonded to MM-atoms.

We modelled the reaction by calculating potential energy surfaces, an approach we have shown to be useful in this and other enzymes.[5,6,14] The potential energy surface for TI formation was calculated by restraining two reaction coordinates. The first was defined as the distance between the attacking water oxygen and the ester carbonyl carbon ($R_A = d[O^4{:}C^1]$, see Scheme 1). The second coordinate modelled abstraction of a proton from the catalytic water by Glu166: it was defined as the difference of the distances between the donating and the accepting oxygen atoms and the transferring proton ($R_B = d[O^4{:}H^5] - d[O^6{:}H^5]$), see Scheme 1). Both reaction coordinates were varied in steps of 0.1 Å and restrained with a force constant of $k = 5000$ kcal mol^{-1} Å^{-2}. At every point of the potential energy surface, the geometry was optimized (with the adopted basis Newton–Raphson[16] (ABNR) method, to a gradient of 0.01 mol^{-1} Å^{-1}). All heavy atoms further than 14 Å from the reaction centre were harmonically restrained to their relaxed crystal coordinates with force constants based on model average *B*-factors.[17] All other atoms were free to move, apart from the restraints applied to the reaction coordinates. The structure of the protein is thus free to respond to changes during the reaction. The energy at every grid point was recalculated, removing any energy contribution from the reaction coordinate restraints. Finally, quantum mechanical energy corrections similar to ref. 6 were performed to obtain the B3LYP/6-31G + (d)//AM1-CHARMM22 surface (for DFT calculations the *Jaguar* program was used[18]). This procedure has been shown to give results comparable to full *ab initio* QM/MM calculations.[19] We have shown[6] it is important in the β-lactamase reaction to account for potential shortcomings of AM1, such as inaccurate basicities.[20] The QM/MM method also allows analysis of changes in electronic distribution during the reaction. We calculated Mulliken charges of QM atoms at the AM1-CHARMM22 QM/MM level. While Mulliken atomic charges have some well-known limitations, changes in charge indicate the most important electronic changes during the reaction (charges are quoted in atomic units, *i.e.* in units of *e*).

The B3LYP/6-31G + (d)//AM1-CHARMM22 potential energy surface (Fig. 1a) indicates a concerted reaction mechanism, *i.e.* the proton transfer is concerted with nucleophilic attack of the water molecule on the AE ester. The lowest energy path from the AE [a0;b0] to the TI [a9;b15] goes approximately through the middle of the surface with a potential energy barrier of 7.2 kcal mol^{-1} (indicated by the energy of the approximate transition state (TS) at [a1;b8]; the TS is the highest energy point along the minimum energy path from the AE to the TI). The height of the barrier for formation of the TI is similar to the barrier for acylation[6] calculated in the same system at the same level (8.7 kcal mol^{-1}). This is consistent with experimental results that show that the rates of acylation and deacylation of TEM1 by benzylpenicillin are of similar magnitude.[4] Pure density-functional theory calculations underestimate barriers for some reactions, in particular for proton transfer, and hybrid DFT methods such as B3LYP are also known to give barriers that are too low in some cases.[21] It may be that the barriers calculated here are a little too low. It should also be remembered that these are potential energy barriers, not free energy barriers. Zero-point, proton tunnelling and entropic effects are not included. Non-chemical steps (*e.g.* binding, conformational changes, product

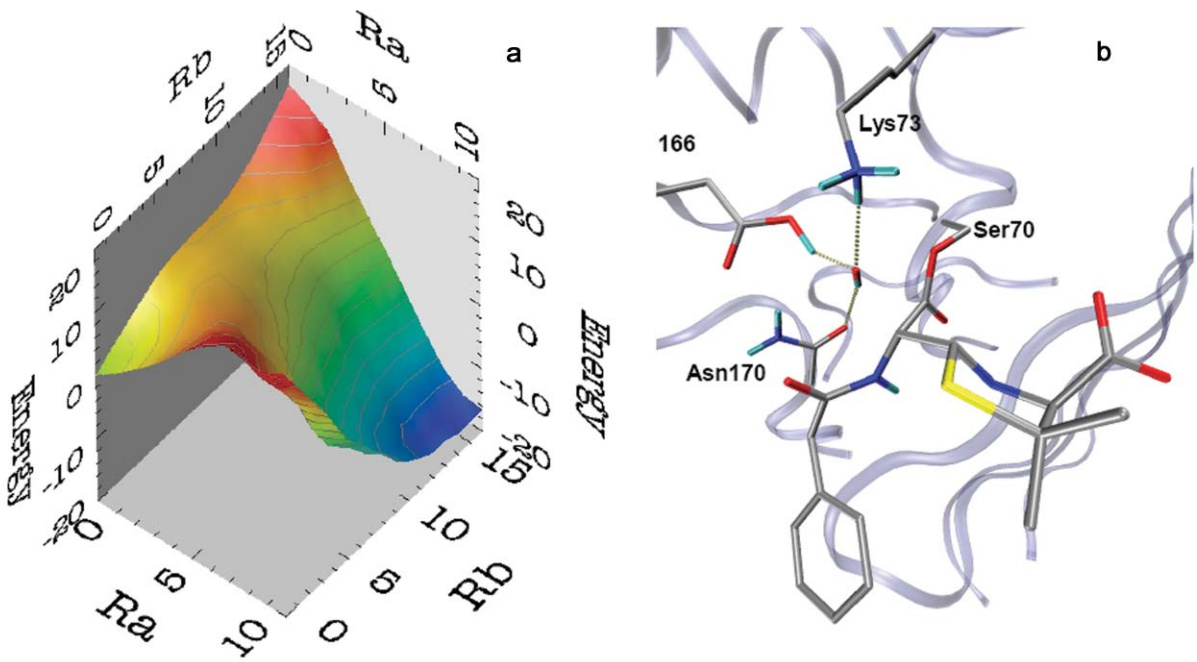

Fig. 1 (a) B3LYP/6-31G + (d)//AM1-CHARMM22 potential energy surface for TI formation in deacylation described by reaction coordinates *Ra* and *Rb* (energies are given relative to the acylenzyme (AE) in kcal mol^{-1}; for clarity the reaction coordinates are labelled with the increment numbers and not with the reaction coordinate values (*e.g.* '0' is the starting point of a particular coordinate); (b) structure of the TS (point [a1;b8] on the surface) showing some important hydrogen bonds [(b) was generated using VMD][23].

release) can also contribute to the overall rate of an enzyme reaction. The barrier calculated here is consistent with (lower than) the experimental activation energy of *ca.* 12 kcal mol^{-1} for deacylation derived from experiment[4] (estimated by transition state theory[22]).

In the TS (Fig. 1b), proton abstraction from the water molecule to Glu166 is almost complete: the distance of the moving proton to the oxygen of Glu166 (H^5–O^6) is 1.10 Å (0.99 Å at the TI), whereas the distance to the water oxygen is 1.40 Å. The distance of the water oxygen to the carbonyl carbon is decreased from 2.41 Å in the AE to 2.30 Å at the TS, indicating that the nucleophilic attack is just beginning. The C^1–O^4 distance (see Scheme 1) shortens continuously from the TS to the TI, where it reaches its equilibrium distance of 1.50 Å.

Analysis of the interaction of the reacting system with the protein environment can identify key groups involved in stabilizing transition states and intermediates in enzymes.[6,14,18,24] The interaction energies of protein residues in the environment (treated by molecular mechanics) with the reacting system (treated quantum mechanically) are calculated for each of the crucial species in the reaction (AE, TS and TI). Residues that significantly stabilize the TS or TI relative to the AE are predicted to have a significant effect on the reaction. These are purely interaction energies, and do not allow for dielectric shielding, so must not be viewed as estimates of effects due to mutation, for example. The aim is not to establish the causes of catalysis (which would require comparison with the equivalent reaction in solution), but simply to identify strongly stabilizing interactions within the enzyme.

The TS and TI are stabilized by the same amino acids but to a different extent. The TI is stabilized by 37 kcal mol^{-1}, whereas the TS is stabilized by 12 kcal mol^{-1}. The same amino acids are important in both cases, so we focus here on the TI, which is stabilized more. Fig. 2a shows the influence of single residues on the stability of the TI, relative to the AE; those identified as most important here (see below) were previously found to contribute in the equivalent step in acylation.[6] This indicates comparable stabilization mechanisms in both reaction steps, which is reasonable, given that the key processes in acylation and deacylation are analogous.

The biggest effects (Fig. 2a) are due to several conserved amino acids, located on the opposite side of the active site to Glu166 (Fig. 2b): Lys234 contributes 15.5 kcal mol^{-1}, Arg244 12 kcal mol^{-1} and Arg275 10 kcal mol^{-1} to the stabilization of the TI (see Fig. 2a). These charged residues compensate for the electronic rearrangement at the active site in deacylation. As in acylation, a proton is transferred to Glu166 during the deacylation step. The negative charge of the Glu166 carboxylate group is thus transferred towards these residues. The atomic charges of the Glu166 carboxylate oxygens in the AE ($O^6 = -0.66$ and $O^7 = -0.66$; see Scheme 1) are lower in the TI ($O^6 = -0.47$ and $O^7 = -0.35$), reflecting the protonation of O^6. The negative charge in the TI is mainly on the oxygens of the AE ester group, whose charges in the TI ($O^3 = -0.74$ and $O^2 = -0.41$) are higher than they were in the AE ($O^3 = -0.46$ and $O^2 = -0.26$). These atoms are closer to the positively charged residues and therefore the electrostatic interaction is improved, which stabilizes the TI. The TI is further stabilized by the so-called oxyanion hole (by 15 kcal mol^{-1}, see Fig. 2a). The oxyanion hole is formed by two backbone peptide bonds (between Met69 and Ser70 and between Gly236 and Ala237; Fig. 2b). The backbone NHs of these two peptide bonds donate hydrogen bonds to the ester carbonyl oxygen, which becomes more negatively charged in the TI. These hydrogen bonds are stronger with the TI (they shorten from 1.67 to 1.79 Å and from 1.96 to 1.91 Å, respectively; hydrogen bond lengths are given throughout as H to acceptor distances). Less obvious is the stabilization of the TI (by 2.1 kcal mol^{-1} relative to the AE) by the conserved Asn132. The sidechain carbonyl oxygen of Asn132 accepts a hydrogen bond from Lys73. This stabilizes the positively charged Lys73 particularly in the TI, in which its salt bridge to Glu166 has been lost. The increased strength of the Lys73–Asn132 interaction is indicated by a slight shortening of the already very short hydrogen bond from 1.70 Å in the AE to 1.66 Å in the TI.

In the TS, the negative charge is mostly on the water oxygen (O^4 has a charge of −0.62 in the TS compared to −0.47 in the AE), and is apparently stabilized by Lys73. Lys73 donates a short hydrogen bond to the water oxygen with a length of 1.9 Å in the TS (decreased from 2.4 Å in the AE). Stabilization of the deacylation TS is likely to be another crucial function of Lys73 (it also has proton shuttle functions in acylation, see ref. 6 and below), and is only possible if it is positively charged (it has been suggested that neutral Lys73 is the base,[9,25] but experiments and calculations support the protonated state).[5,6,26] This hydrogen bond is very likely to lower the barrier and might be the reason why this transition state structure could not be found in a QM/MM study using neutral Lys73.[27] The importance of Lys73 for deacylation is demonstrated by experimental studies of a K73 mutant, for which

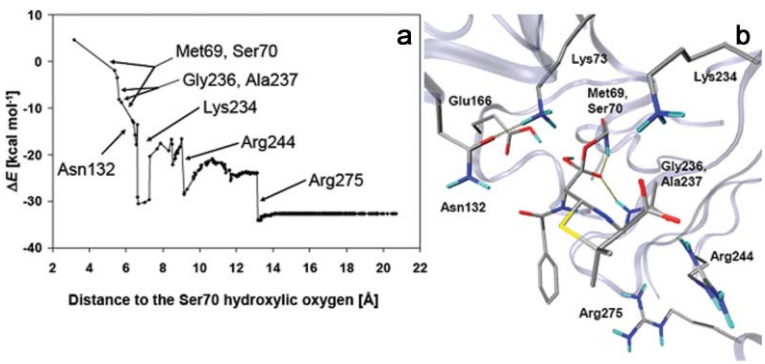

Fig. 2 (a) Contributions of individual MM residues to the QM/MM energy difference between the tetrahedral intermediate and the acylenzyme (E(TI) − E(AE)), showing residues that stabilize the TI relative to the AE; (b) structure of the tetrahedral intermediate showing important stabilizing residues.

decreased deacylation rates were observed.[4,28] The importance for deacylation of Lys73 (in stabilizing the TS) that we find is consistent with experiment.

Combined with our previous findings for the acylation mechanism,[6] we are now able to present the energy profile for the whole reaction from the Michaelis complex to the formation of the TI for deacylation (TI2). The energy profile for the cleavage of benzylpenicillin by TEM1 to the deacylation TI is shown in Fig. 3. The potential energy profile indicates the exothermic character of the enzymic reaction, with an energy decrease from the substrate complex to the deacylation TI of around 47 kcal mol^{-1}. This energy change may be overestimated somewhat (*e.g.* due to long-range electrostatic interactions), but the profile is in line with proposals that well-evolved enzymes that catalyse thermodynamically favourable reactions should have overall descending energy profiles.[29] The results indicate that the various steps in antibiotic breakdown have comparable barriers, with no step being clearly rate-limiting. The step with the highest barrier in acylation is formation of the first tetrahedral intermediate, TI1 (TS1 is the transition state for this step, with an energy relative to the Michaelis complex of 8.7 kcal mol^{-1}). The second process in acylation forms the acylenzyme (AE), by proton transfer from Glu166 to the nitrogen of the thiazolidine ring, involving Lys73 and Ser130 as proton shuttle residues.[6] This has a slightly lower barrier (TS2 is 7.1 kcal mol^{-1} higher in energy than TI1), similar to the barrier for deacylation (TS3 is 7.2 kcal mol^{-1} above the AE). These results suggest that k_{cat} depends on several reaction processes with similar barriers, instead of one dominant rate-determining step. Formation of the tetrahedral intermediate is likely to have the highest barrier in both steps.[6]

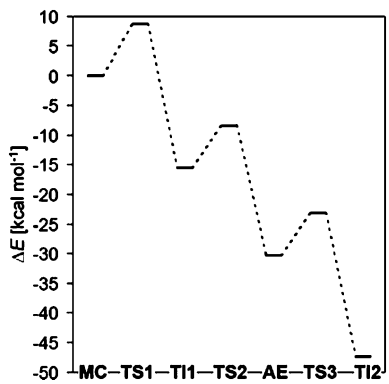

Fig. 3 B3LYP/6-31G + (d)//AM1-CHARMM22 QM/MM energy profile for the cleavage of benzylpenicillin by the TEM1 class A β-lactamase. MC is the Michaelis (substrate) complex; TS1, TI1, TS2, are transition states and the tetrahedral intermediate for acylation; TS3 and TI2 are the transition state and the tetrahedral intermediate for deacylation.

In conclusion, the results here demonstrate how the entire complex sequence of reactions can take place efficiently in the active site, without major structural rearrangement. They identify all the catalytic groups and key interactions. The calculated barrier for formation of the tetrahedral intermediate in deacylation (7.2 kcal mol^{-1}) is consistent with the experimental reaction rate. The results provide a structurally detailed mechanism, and complete energy profile, for the reaction starting from the substrate (Michaelis) complex, through to formation of the TI for deacylation. The results show the importance of including (at least key parts of) the protein environment to obtain reasonable energetics for the enzyme reaction. The finding here that tetrahedral intermediate formation has the highest barrier in deacylation is in agreement with DFT calculations on small models,[30] and also QM/MM modelling of the deacylation reaction of a serine protease (elastase).[31]

The active site of the class A β-lactamase is clearly well adapted to allow electronic changes during formation of the tetrahedral intermediate. Firstly, Lys73 stabilizes the transition state by donating a hydrogen bond to the hydroxide-like water molecule, lowering the barrier for the deacylation reaction. Secondly, the enzyme compensates very effectively for the increase of negative charge on the oxygens of the acylenzyme/tetrahedral intermediate during the reaction. Stabilization is provided by the charged amino acids Lys234, Arg244 and Arg275, the residues forming the oxyanion hole, and Asn132 (all of which are conserved within the class A β-lactamases). Almost identical stabilization mechanisms (involving the same residues) are found for the formation of the tetrahedral intermediate in the acylation step.[6] This suggests that the development of the enzyme's active site in the evolution has benefited from the similarity of the tetrahedral intermediates in both reaction steps. The similarity is based on the initiation of each reaction step: the abstraction of a proton from the nucleophile by Glu166, and the relocation of the general base's negative charge in the active site to a more central position (to atoms of the carbonyl group of the β-lactam substrate). The resulting similar distributions of charges in the active site during the reactions have allowed an economical optimization of the active site for the stabilization needed to catalyse both acylation and deacylation. These detailed insights into the stabilizing interactions of specific residues could assist the design of new, more stable, antibiotics (*e.g.* by creating interactions with crucial amino acid functionalities and so prevent the stabilizing interactions), which then would ideally affect acylation and deacylation. This mechanistic knowledge may therefore be useful in the development of new drugs to overcome bacterial antibiotic resistance.

Acknowledgements

A.J.M. and J.C.H. thank the Royal Society for a visiting fellowship (2004/R2-EU) for J.C.H. and the Deutscher Akademischer Austauschdienst (DAAD) for a short term fellowship for J.C.H. under contract number PKZ D/04/23634. A.J.M. also thanks BBSRC, EPSRC, The Wolfson Trust, The Royal Society and the IBM High Performance Computing Life Sciences Outreach Programme for support.

References

1 M. L. Cohen, *Science*, 1992, **257**, 1050–1055; H. C. Neu, *Science*, 1992, **257**, 1064–1073; J. Davies, *Science*, 1994, **264**, 375–382.
2 Amino acid numbering according to R. P. Ambler, A. F. W. Coulson, J.-M. Frère, J.-M. Ghuysen, B. Joris, M. Forsman, R. C. Levesque, G. Tiraby and S. G. Waley, *Biochem. J.*, 1991, **276**, 269–272.
3 A. Matagne, J. Lamotte-Brasseur and J.-M. Frère, *Biochem. J.*, 1998, **330**, 581–598.
4 R. M. Gibson, H. Christensen and S. G. Waley, *Biochem. J.*, 1990, **272**, 613–619.
5 J. C. Hermann, L. Ridder, A. J. Mulholland and H.-D. Höltje, *J. Am. Chem. Soc.*, 2003, **125**, 9590–9591.
6 J. C. Hermann, C. Hensen, L. Ridder, A. J. Mulholland and H.-D. Höltje, *J. Am. Chem. Soc.*, 2005, **127**, 4454–4465.
7 C. Oefner and F. K. Winkler, *Nature*, 1990, **343**, 284–288.

8 H. M. Berman, J. Westbrook, Z. Feng, G. Gilliland, T. N. Bhat, H. Weissig, I. N. Shindyalov and P. E. Bourne, *Nucleic Acids Res.*, 2000, **28**, 235–242.
9 N. C. J. Strynadka, H. Adachi, S. E. Jensen, K. Johns, A. Sielecki, C. Betzel, K. Sutoh and M. N. G. James, *Nature*, 1992, **359**, 700–705.
10 M. J. Field, P. A. Bash and M. Karplus, *J. Comput. Chem.*, 1990, **11**, 700–733.
11 B. R. Brooks, R. E. Bruccoleri, B. D. Olafson, D. J. States, S. Swaminathan and M. Karplus, *J. Comput. Chem.*, 1983, **4**, 187–217.
12 A. D. MacKerell, D. Bashford, M. Bellot, R. L. Dunbrack, J. D. Evanseck, M. J. Field, S. Fischer, J. Gao, J. Guo, S. Ha, D. Joseph-McCarthy, L. Kuchnir, K. Kuczera, F. T. K. Lau, C. Mattos, S. Michnick, T. Ngo, D. T. Nguyen, B. Prodhom, W. E. Reiher, B. Roux, M. Schlenkrich, J. C. Smith, R. Stote, J. Straub, M. Watanabe, J. Wiorkiewicz-Kuczera, D. Yin and M. Karplus, *J. Phys. Chem. B*, 1998, **102**, 3586–3616.
13 M. J. S. Dewar, E. G. Zoebisch, E. F. Healy and J. J. P. Stewart, *J. Am. Chem. Soc.*, 1985, **107**, 3902–3909.
14 L. Ridder, A. J. Mulholland, I. M. C. M. Rietjens and J. Vervoort, *J. Am. Chem. Soc.*, 2002, **122**, 8728–8738; L. Ridder, I. M. C. M. Rietjens, J. Vervoort and A. J. Mulholland, *J. Am. Chem. Soc.*, 2002, **124**, 9926–9936; A. Lodola, M. Mor, J. C. Hermann, G. Tarzia, D. Piomelli and A. J. Mulholland, *Chem. Commun.*, 2005, **35**, 4399–4401; C. Hensen, J. C. Hermann, K. Nam, S. Ma, J. Gao and H. D. Höltje, *J. Med. Chem.*, 2004, **47**, 6673–6680.
15 N. Reuter, A. Dejaegere, B. Maigret and M. Karplus, *J. Phys. Chem. A*, 2000, **104**, 1720–1735.
16 R. H. Boyd, *J. Chem. Phys.*, 1968, **19**, 2574–2583.
17 C. L. Brooks, III and M. Karplus, *J. Mol. Biol.*, 1989, **208**, 159–181.
18 *Jaguar 4.1*, Schrödinger, Inc., Portland, OR, 1991–2000.
19 K. E. Ranaghan, L. Ridder, L., B. Szefczyk, W. A. Sokalski, J. C. Hermann and A. J. Mulholland, *Mol. Phys.*, 2003, **101**, 2695–2714; K. E. Ranaghan, L. Ridder, B. Szefczyk, W. A. Sokalski, J. C. Hermann and A. J. Mulholland, *Org. Biomol. Chem.*, 2004, **2**, 968–980.
20 E. Lewars, in *Computational Chemistry*, Kluwer Academic Publishers, Dordrecht, 2003, pp. 339–382.
21 T. Hayashi and S. Mukamel, *J. Phys. Chem. A*, 2003, **107**, 9113–9131; S. Morpurgo, M. Brahimi, M. Bossa and G. O. Morpurgo, *Phys. Chem. Chem. Phys.*, 2000, **2**, 2707–2713; A. Dkhissi, L. Adamowicz and G. Maes, *J. Phys. Chem. A*, 2000, **104**, 2112–2119; M. Loszynski, D. Rusisnka-Roszak and H.-G. Mack, *J. Phys. Chem. A*, 1989, **102**, 2899–2903.
22 M. Garcia-Viloca, J. Gao, M. Karplus and D. G. Truhlar, *Science*, 2004, **303**, 186–195.
23 W. Humphrey, A. Dalke and K. Schulten, *J. Mol. Graphics*, 1996, **14**, 33–38.
24 A. J. Mulholland, A. J. and W. G. Richards, *Proteins*, 1997, **27**, 9–25.
25 P. Swarén, L. Maveyraud, V. Guillet, J. M. Masson, L. Mourey and J. M. Samama, *Structure*, 1995, **3**, 603–613.
26 J. Lamotte-Brasseur, R. Wade and X. Raquet, *Protein Sci.*, 1999, **8**, 404–409; X. Raquet, V. Lounnas, J. Lamotte-Brasseur, J. M. Frère and R. Wade, *Biophys. J.*, 1997, **73**, 2416–2426; C. Damblon, X. Raquet, L.-Y. Lian, J. Lamotte-Brasseur, E. Fonze, P. Charlier, C. K. R. Gordon and J. M. Frère, *Proc. Natl. Acad. Sci. U. S. A.*, 1996, **93**, 1747–1752; S. O. Meroueh, G. Minasov, G. W. Lee, B. K. Shoichet and S. Mobashery, *J. Am. Chem. Soc.*, 2003, **125**, 9612–9618; M. Nukaga, K. Mayama, A. Hujer, R. A. Bonomo and J. R. Knox, *J. Mol. Biol.*, 2003, **328**, 289–301.
27 E. J. Lietz, D. K. Truher, M. J. Hokenson and A. L. Fink, *Biochemistry*, 2000, **39**, 4971–4981.
28 R. Castillo, E. Silla and I. Tunon, *J. Am. Chem. Soc.*, 2000, **124**, 1809–1816.
29 W. J. Albery and J. R. Knowles, *Angew. Chem., Int. Ed. Engl.*, 1977, **16**, 285–293; J. Stackhouse, K. P. Nambiar, J. Burbaum, D. M. Stauffer and S. A. Benner, *J. Am. Chem. Soc.*, 1985, **107**, 2757–2763.
30 Y. Fujii, M. Hata, T. Hoshino and M. Tsuda, *J. Phys. Chem. B*, 2002, **106**, 9687–9695.
31 M. Hopf and W. G. Richards, *J. Am. Chem. Soc.*, 2004, **126**, 14631–14641.

